Cosmic Ray Detectors

Carlo Morello[1]

INAF – Istituto di Fisica dello Spazio Interplanetario
Corso Fiume 4
10133 Torino, Italy
E-mail: c.morello@ifsi-torino.inaf.it

The observation of the cosmic radiation began almost 100 years ago, soon after the balloon flight of Victor Hess in 1912. Since then, different experimental techniques have been developed and applied to detect and to understand the nature and the properties of such energetic particles. The paper is devoted to present the main methods used to detect the cosmic rays by satellite and balloon born experiments as well as by ground based arrays.

---

[1]   Speaker

1. Introduction

Cosmic rays are high energy charged and neutral particles, originated in outer space and travelling at nearly the speed of light, striking the Earth from all directions. Most cosmic rays are nuclei of atoms, ranging from the lightest to the heaviest elements, but cosmic rays also include high energy photons, electrons, positrons and other subatomic particles [1].

Cosmic rays cover a very wide range of energies from roughly 1000 eV (1 eV ≈ 1.6 x 10^{-19} Joule) to more than 10^{20} eV. The detectors used to study cosmic ray physics need therefore to cover more than 16 decades in energy and this has a reflection on the detection techniques.
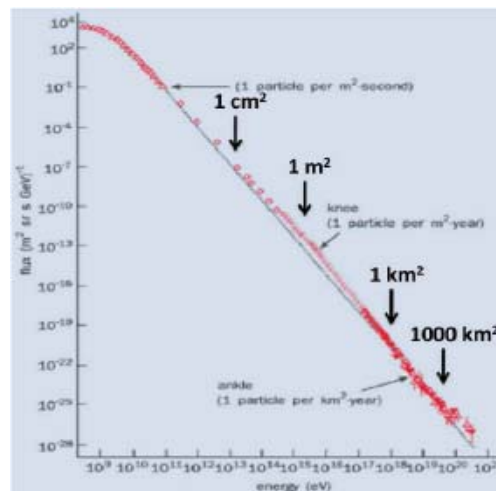

Figure 1. Cosmic ray primary intensity as a function of energy. The sensitive area needed to observe 1 event/month is indicated.

The energy spectrum of all cosmic-ray particles is shown in Fig. 1: it falls steeply as a function of energy, decreasing by about a factor 500 per decade in energy. The flux decreases from more than 1000 particles per second and square meter at GeV energies to about one particle per m^2 and year at a PeV, and further to less than one particle per km^2 and century above 100 EeV (1 keV = 10^3 eV, 1 MeV = 10^6 eV, 1 GeV = 10^9 eV, 1 TeV = 10^{12} eV, 1 PeV = 10^{15} eV, 1 EeV = 10^{18} eV, 1 ZeV = 10^{21} eV). The strong decrease in flux poses a big challenge to the dimensions and the running times of the experimental installations. Balloon and satellite born detectors operate at an altitude above 15 km where they can detect the interaction of the primary particle inside the detector. Such instruments are limited in weight and detection area and therefore also limited in the energy range they can measure. Due to low fluxes, the maximum primary energy that can be measured by means of "direct" observations is of the order of 10^{14} – 10^{15} eV. Above these energies the observations are performed by exploiting the cascades induced in atmosphere by the primary interactions. This method requires large detection areas to collect a suitable number of particles in a reasonable time. Such detectors are installed at ground level, the atmospheric depth being related to the target primary energy (the

total atmospheric depth is ~ 1000 gr/cm^2) , or underground/underwater for neutrino detection. At the highest energies ground level apparatuses with large detection area require observation times of the order of 10-20 years, long term stability of the detectors and the need for monitoring and maintenance of arrays quite often located in peculiar geographical sites (i.e. mountain altitude, Argentinean pampa, Antarctica).

The investigations toward what later on have been recognized as cosmic rays have been driven by the curiosity of explaining the discharge of the electroscopes, believed to be due to a natural ionizing radiation of the Earth. The experiment performed by T. Wulf in 1910 proved that attenuation in air of the unknown radiation was lower than expected. Cosmic rays were then discovered in 1912 by Victor Hess, who found that an electroscope discharged more rapidly as he ascended in a balloon flight. He attributed this to a source of radiation entering the atmosphere from above. For some time it was believed that the radiation was electromagnetic in nature (hence the name cosmic "rays"), however, during the 1930's it was found that cosmic rays must be electrically charged because they are affected by the Earth's magnetic field [2,3,4]. The birth of modern arrays is related to the development of time resolving single particle detectors as Geiger counters and electronic circuits like the Rossi coincidence. Cloud chambers and nuclear emulsions represent examples of tracking and high resolution detectors first used for particle physics but that have marked the development of cosmic ray detectors [5]. The development of scintillators and of Cherenkov light detectors have brought into the field new tools for high precision measurements and devices allowing to cover large collecting areas.

The Earth magnetic field played a fundamental role in the first understanding of the primary radiation, on the separation of charged and neutral particles and on the determination of the predominant charge. Pioneer works in using the Earth magnetic field as a magnetic analyzer were performed by J. Clay, A.H. Compton, T.H. Johnson, L.W. Alvarez and B. Rossi.

2. Space detectors for cosmic rays

The basic detector scheme used to allow particle identification and primary energy determination in space born experiments is shown in Fig. 2. The arrival directions are limited inside a given opening angle by a telescope allowing to know the particle trajectory inside the following calorimeter; the anticoincidence system guarantees the full containment of the energy released by the incident particle. In this way the geometry is completely known.

The energy losses of the electromagnetic (e.m.) interactions of charged particles are given by the Bethe – Block expression [6] (β particle velocity, Z particle charge) :

$$-\frac{dE_0}{dx} \approx 2 \cdot \frac{Z^2}{\beta^2} \cdot log(f(Ip,\beta))\frac{MeV}{gr \cdot cm^{-2}}$$

The particle charge can be deduced by means of combined measurements of the kinetic energy E_0 and of the energy loss inside a thin scintillator. At non relativistic energies the particle mass can be identified by the relation: $1/\beta^2 \propto M/E_0$ [7].
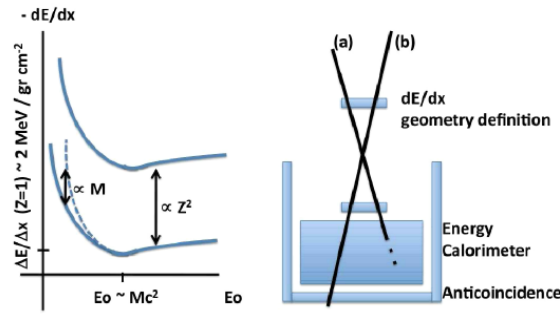
Figure 2. Principle of the detectors used in space experiments for energy measurements and particle identification [8].

Above the critical energy to radiate or above the π^0 production threshold the primary particle produces electromagnetic cascades by subsequent processes of electron bremmstrahlung and photon pair production. Radiation processes dominate and the e.m. cascade develops till the average energy is larger than the critical energy E_c. Below E_c the cascade is absorbed due to the energy losses by collision and the energy is converted inside the detector in photons or in other measurable quanta by the measuring devices.

As the quoted effects depend on the square of the electric charge (Z^2), most of the space detector provide on board a magnet and the magnetic deflection can add an additional energy measurement [9,10].

In the described "calorimetric" measurements the energy loss inside the detector is converted in "quanta". The number n of collected quanta depends on the energy E_q needed for each quantum and on the collection efficiency ε of the detecting instruments. Given E_0 the energy of the incoming particle, the number of detected quanta is: $n = \varepsilon E_0/E_q$. The resolution is dominated by Poisson fluctuations and is: $\sigma(E_0)/E_0 = \sqrt{(E_q/ \varepsilon E_0)}$. The resolution improves with increasing primary energy and for detector devices with low E_q (i.e. semiconductors). Typical energy resolution in this kind of direct measurements can be of the order of 10% over the square root of the primary energy E_0 expressed in MeV [11,12].

At high primary energies, when the cascade cannot be contained the number of particles at different depth is sampled by interleaving sensitive low density material and absorbing material with low critical energy and short radiation length. The cascade and the primary energy are reconstructed from the obtained number of particles at different depths. Depth in an absorber is measured in units of lengths x density and therefore in gr/cm^2.

First measurements of high energy galactic radiation based on such principle were performed by means of a direct space experiment in the 1960' by Grigorov et al. [13] exploiting calorimeters aboard of the Proton satellites. In the Proton case the energy resolution was about 20% at ~ 30 GeV. More recently, such measurements have been realized by balloon born long flying electronic detectors like ATIC [14] and CREAM [15].

Classical energy measurements can also be performed by using stacks of emulsion chambers [16, 17].

Gamma rays are not deflected by the galactic magnetic field and their detection provide direct information on the source. When interacting with the detector, γ-rays produce electrons by means of the photoelectric effect, Compton scattering and electron-positron pair production. Pair production is the dominant effect at high energies and the measurements of the energy loss is obtained through the calorimetric measurement of the cascade. The arrival direction measurements are normally performed with an accuracy of ~ 1° in the GeV region through tracking detectors as gas chambers or semiconductor devices. The rejection power of the charged cosmic rays, because of the different fluxes, require anticoincidence systems capable of shielding the γ-ray detector in all directions [18, 19, 20]

3. Ground Based Particle Detectors

At energies of the order of 10^{15} eV the number of events (see Fig.1) is too low for space experiments and besides the increasing limitations in energy determination, the sensitive area of the detectors does not allow the study of the high energy part of the cosmic ray spectrum. The measurements are performed by means of ground based arrays exploiting the Extensive Air Showers (EAS) technique and covering large detection areas.
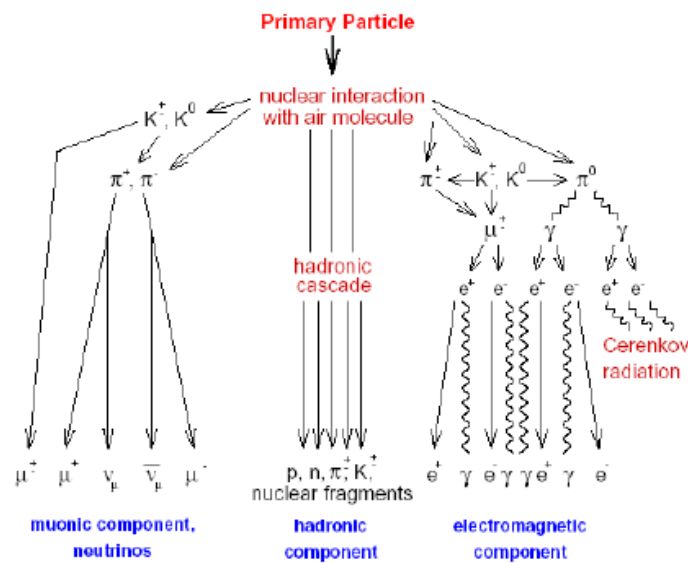

Figure 3. Scheme of the development of Extensive Air Showers [22]

An Air Shower is a cascade of particles generated in atmosphere by the interaction of a primary cosmic ray nucleus or photon characterized by multiple production of secondary particles (pions, kaons,…as shown on Fig. 3).

The shower cascade consists of three components: electromagnetic, muonic and hadronic. The neutral pions decay into gammas, feeding the electromagnetic component via the production of pairs of electrons and positrons. Above the critical energy (E_c = 80 MeV in air), the electrons loose their energy by radiation and contribute to the fraction of gamma in the cascade. Most of the shower energy is therefore dissipated by ionization losses by electrons and

positrons. Secondary kaons decay in $\pi^{+/-}$ interacting or decaying in muons or neutrinos, the hadronic component consisting mainly of nuclear fragments.

The number of secondary particles multiplies reaching a maximum value at a given atmospheric depth (~ 10^6 particles at atmospheric depth of 600 gr cm^{-2} for 10^{15} eV) and then attenuates when most of the particles go below the energy threshold to continue the particle production. The characteristics of the cosmic ray cascades in atmosphere depend on the nature of the primary. However their lateral distribution at the observation level is related to the Coulomb scattering spreading the particles of the cascade over large distances from the shower axis. The typical distance from the shower axis is given by $R_M = E_s/E_c X_0$, with $E_s \approx 21$ MeV. R_M is called Moliere radius and is about 75 m at sea level.

Shower propagate downward into the atmosphere and the particles are sampled at ground level from detectors like scintillation counters by means of the sampling technique.
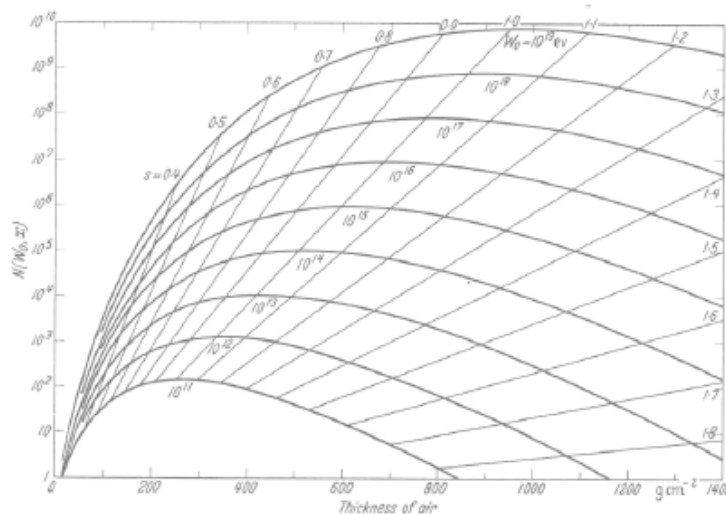

Figure 4. Longitudinal development of electromagnetic cascades in atmosphere

In each detector R of surface A and thickness d < mean free path, a signal S(R) proportional to the energy loss is recorded. If S_m is the signal due to a single trough going particle, $N_{ch} = S(R) / S_m$ gives the number of particle crossing the detector and N_{ch}/A provides the particle density at the given position of the detector. Knowing the densities in different locations we can fit the core position, the slope of the lateral distribution function and the total number of particles in the shower, which is related to the primary energy. If we assume 10^5 – 10^6 shower particles at the observation level distributed over an area given by the Moliere radius R_M, we obtain an average density of few particles per square meter. The described sampling technique allows to realize collecting areas much larger than the sensitive areas as exploited by all EAS arrays [25, 26, 27, 28, 29, 30, 31].

The study of the muonic component plays an important role in the study of the chemical primary composition. While e. m. cascades develop and are then absorbed after a given atmospheric depth, muons are practically not attenuated in atmosphere because of their radiation

length ($1.6 \cdot 10^6$ gr/cm^2). As the electron radiation length is 37.7 gr/cm^2 the difference in the radiation length provides the possibility of absorbing the e.m. component by means of shielding materials of a sufficient thickness without affecting the muon component. Muons with energy lower than GeV decay and do not reach the ground level, while higher energy muons are not significantly affected by the Coloumb scattering and their lateral distribution at the observation level is mainly due to the transverse momentum at the EAS production. Typical muon distance from the shower axis is of the order of 200 m.

The detection on the same events of the e.m. and muon components provide an important tool for primary composition studies. The tool is based on the assumption that a cascade produced by a nucleus of mass A is equivalent to the superposition of A cascades generated by a primary proton. The observable quantities N_e and N_μ, for showers detected after the shower maximum are given by: $N_e \propto A \cdot (E_0/A)\alpha$ and $N_\mu \propto A \cdot (E_0/A)\beta$, $\alpha \approx 1.2$ and $\beta \approx 1.2$. As the primary energy is not measured, the relationship between the observables is: $N_\mu \propto A^{1- \beta/\alpha} \cdot N_e^{\beta/\alpha}$ corresponding to $N_\mu \propto A^{0.2} \cdot N_e^{0.8}$ for the quoted values. As a function of the atmospheric depth the number of muons ranges from 1% to 10% of the electron component and is about a factor 2 larger for a primary iron nuclei than for a primary proton.

The signal corresponding to the loss of energy of a single minimum ionizing particle inside the individual detectors of the array has to be continuously calibrated and monitored to keep its fluctuations at poissonian level, as this information is used into the shower reconstruction procedure. The all-particle lateral distribution is obtained from the particle density measurements at different location. The total number of particles at the observation level and the geometrical position on ground of the shower core are obtained by fitting a theoretical expression of the lateral distribution of the charged particles. The arrival direction of the showers is obtained by measuring the particle arrival time in each individual detector. The arrival delays of the particles and the distance among the detectors are used to obtain the arrival angles. As a first approximation, the shower front can be assumed to be flat and with negligible thickness. The thickness of a real shower disk introduces an uncertainty of the order of the degree.

If the detector has a thickness greater than the radiation length, the e.m. component looses all its energy, while the muon component usually crosses the whole detector and releases an energy proportional to the detector thickness. In this case the reconstruction procedure has to take into account that the detectors contribute with different weights.

In case the distance among the detectors is greater than the Moliere radius, it can be convenient to derive the particle density at a given core distance as this reduces the uncertainties. The optimum distance from the shower core at which to derive the particle density depends on the detector configuration. Such distance was 600 m for the Haverah Park array and is 1000 m for the Pierre Auger Observatory.

4. Ground Based Optical Detectors

The study of the high energy cosmic rays can also be performed by observing the longitudinal development of the cascades in atmosphere exploiting the Cherenkov and fluorescence light emitted in atmosphere by the charged secondary particles.

The Cherenkov radiation arises when a charged particle moves in a material at a speed v > c/n, being c the speed of light and n the refraction index. The coherent wavefront is emitted at an angle $\cos \theta = 1/ \beta n$ with $\beta = v/c$. The particle's threshold speed for Cherenkov emission is $\beta = 1/n$. The maximum emission angle is $\theta = \arccos (1/n)$. The number of photons emitted per unit length is $dN/dl = 2\pi\alpha (1/\lambda_2 - 1/\lambda_1) \sin^2\theta$. In air the Cherenkov energy threshold is 21 MeV for electrons and 4.3 GeV for muons; the maximum emission angle is 1.3° and dN/dl = 23 ph/m at sea level for 350 < λ < 500 nm, β = 1 and Z =1.

The isotropic fluorescence emission in atmosphere is mainly due to nitrogen excitation. The emission is concentrated in a few lines between 300 and 480 nm, the emission is ~ 4.8 ph/m at sea level.

Cherenkov and fluorescence detectors are used to investigate different energy intervals: small angle directional Cherenkov detectors around 10^{12} eV, large angle directional Cherenkov detectors around 10^{15} eV and fluorescence detectors around 10^{17} eV. While the amount of the Cherenkov photons is completely understood, the amount of energy loss converted into the "fluorescence photon yield" has still some uncertainties. The uncertainty, including the dependence from air temperature and pressure, amounts to about 15%.

Such observations are strongly dependent from the night sky conditions and require the monitoring of the atmosphere during the measurements to reduce the uncertainties and limitations of the measurements. The duty cycle is of the order of 10% as observations can be performed only in clear moonless nights.

As optical detectors use the atmosphere as "calorimeter", they can provide energy measurements quite independent from calculations including assumptions on the hadron interaction properties. The direct observation of the EAS cascade by fluorescence detectors allows the measurement of the depth of the shower maximum, which is related to the nature of the primary. In case of Cherenkov detectors, the depth of shower maximum can be obtained by converting the light lateral distribution in the longitudinal shower development.

4.1 Atmospheric Cherenkov Detectors

A main problem of the ground based particle arrays is the impossibility to discriminate the charged particle of the cosmic radiation. The methods used to improve the sensitivity to the primary gamma component include the detection of the muon component, the study of the lateral distribution and arrays built at high altitude and with continuous layers of sensitive areas to reduce the primary energy threshold and to connect the ground based gamma ray observations with the satellite experiments [32, 33]. Main characteristics of the atmospheric Cherenkov radiation are: 1) the Cherenkov light lateral distribution extends till large distances from the shower axis (~ 100 m) and it is therefore possible to realize large detection areas; 2)
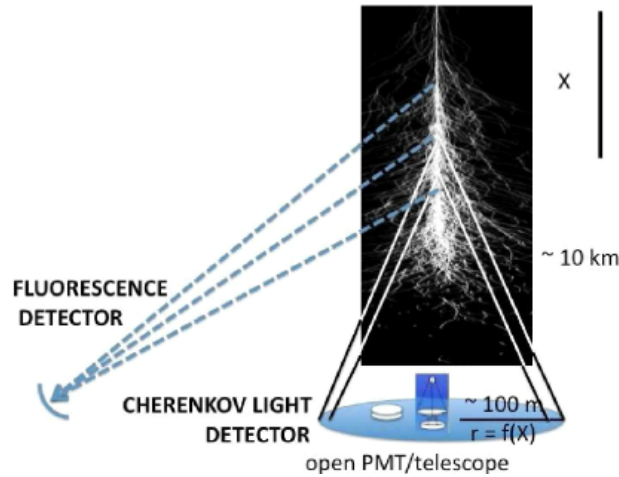
Figure 5. Scheme of atmospheric fluorescence and Cherenkov detectors [8]

the light angular distribution is very narrow and the arrival direction of the primary particle is conserved; 3) the temporal structure of the signal is limited to few nanoseconds and this allows to integrate the night sky background ($B \approx 10^{12}$ ph.m^{-2} sec^{-1} sr^{-1}) for a short time interval. Atmospheric Cherenkov measurements are performed against the fluctuations of the night sky background limiting the energy threshold of the detectors. The number of background photons are given by : $n_{ph} = B \, A \, \Omega \, \varepsilon \, \tau$, being A the mirror area ≈ 100 m^2, Ω the solid angle $\approx 10^{-3}$ sr, ε the photocathode quantum efficiency $\approx 0,2$ and τ the integration time ≈ 10 ns. The number of Cherenkov photons is given by : $N_{ph} = N \, A \, \varepsilon$, being N the number of Cherenkov photons m^{-2} inside the solid angle Ω at a given distance r ≈ 100 m from the shower axis ≈ 50 ph/m^2 ·TeV. The energy threshold is determined by the relation $N_{ph}/\sqrt{n_{ph}} > k$. Assuming k = 10, an energy threshold of 200 GeV is obtained to be compared with energy threshold of 50 – 100 GeV for the existing detectors [34, 35,36].

The field of ground-based gamma-ray astronomy has been pioneered by the work of the Whipple collaboration, which successfully discovered the first source of TeV gamma-rays, the Crab Nebula, in 1989 almost 20 years ago [37]. The discrimination power of the last generation of Cherenkov telescopes between Cherenkov signals generated by charged particle and primary gammas is due to the shape and orientation of the Cherenkov image obtained by imaging cameras with pixels field of view of the order of 0.1°.

5. High Energy Neutrino Detectors

Neutrino detectors, because of the very low signal rates, have to be shielded against the charged cosmic rays, acting in this kind of measurements as a source of background. For this reason neutrino detectors have to be built deep underground or underwater.

The neutrino cross section $\sigma(\upsilon_\mu) \approx 6.7 \, 10^{-36}$ E/TeV cm^2/n gives a probability of interaction of P $\approx 4 \cdot 10^{-7}$ E/TeV for 1 km depth of water and this requires detectors with very large active volumes. The interaction channel $\upsilon_\mu + N \rightarrow N + X + \mu$ is relevant for the neutrino detection, as

the interaction point can be detected through the hadron/e.m. cascade and the through going muon having a track length of about 2 km in water. The muon-neutrino angle is $\theta_{\upsilon\mu} \approx 1.5°$ / $\sqrt{(E_{\upsilon}/TeV)}$ and therefore by reconstructing the muon direction it is possible to reconstruct also the neutrino arrival direction. Moreover, the track length of the trough going muon allows to extend the detector sensitivity well outside the physical volume of the detector.

In the case of under water or under ice detectors, the shielding material is also the medium in which Cherenkov light is produced and detected by arrays of photomultipliers. An ultra relativistic particle produces in water about 400 photons/cm and the emission angle is 42°. Assuming a photocathode area of 0.1 m^2 and a quantum efficiency of 20% at a distance of 50-100 m from the interaction point, we can have 1 photoelectron if the attenuation track length of the medium is $\approx$ 50 m. The transparency of the medium in the visible-blue spectral region of the photocathodes is therefore a crucial property to choose the site of the measurements and it has to be clean from additional sources of background like radioactivity or bioluminescence

The first project to explore the possibility of high energy neutrino detection by deploying string of photomultipliers deep in the sea has been the DUMAND project [38]. At present, different experiments are deployed in different sites as lake water [39], mediterranean sea [40, 41, 42] and in antarctic ice [43].

6. Radio and Acoustic Detectors

In the last few years the technical developments have made possible the detection of already known and detectable effects as the radio emission from Extensive Air Showers in atmosphere and of acoustic frequency in water or ice.

Radio emission from EAS was first detected in 1965 by J. Jelley et al.. The syncrotron radiation emitted by the secondary electrons and positrons of the cascade in the Earth magnetic field extends up to the GHz region but the optimal frequency region is limited around 100 MHz because of the spread of the shower particles. Due to technical difficulties this EAS detection method was abandoned soon after its discovery in the seventies. Recently, the method has been used by the LOPES Collaboration [44] operating at the KASCADE Grande site in the energy interval 10^{15} -10^{18} eV and by the CODALEMA Collaboration [45].

The Lopes results show that the signal depend on the angle between the shower axis and the Earth magnetic field, thus confirming that the emission is a geomagnetic effect. The measurements also show a good correlation of the radio signal with the muon number measured by the KASCADE array and trough this a good correlation with the primary energy. Tests and calibration are performed in the energy interval $> 10^{17}$ eV at the site of the Pierre Auger Observatory in Argentina showing a good detection efficiecy.

The acoustic emission by the cascades heating the medium and generating a pressure wave have been detected at accelerators and the response is linear with energy. In water and ice the cascades are of the order of cm and for energy release above 10^{15} eV the pressure wave can be detected with the present techniques. The emission frequencies are of the order of 10 KHz: since the attenuation length in water is of the order of km, the technique is interesting as the effect can be detected far away from the emission area. Tests are on going in the lake Baikal.

References

[1] M.S.Longair, *High Energy Astrophysics,* Cambrige University Press (1992)

[2] B. Rossi, *Cosmic Rays,* McGraw-Hill (1964)

[3] B.Rossi, *High Energy Particles,* Prentice-Hall (1952)

[4] L.Leprince-Ringuet, *Les Rayons Cosmiques,* Albin Michel Paris (1945)

[5] W.R.Leo, *Techniques for Nuclear and Particle Physics Experiments,* Springer, Berlin (1994)

[6] Review of Particle Physics, *Physics Letter B*, 592 (2004)

[7] CRIS, http://www.srl.caltech.edu/ACE/CRIS_SIS/cris.html

[8] A.Altamirano, G.Navarra, *Detectors of Cosmic Rays, Gamma Rays and Neutrinos,* Third School on Cosmic Rays and Astrophysics (2008)

[9] PAMELA, http://pamela.roma2.infn.it/index.php

[10] AMS, http://ams.cern.ch/AMS/Description/overview.html

[11] K. Pretzl, *J. Phys. G: Nucl. Part. Phys.,* 31 (2005) R133

[12] U. Amaldi, *Physica Scripta,* 23 (1981) 409

[13] N.L. Grigorov et al, *Sov. Journal Nucl.Phys.,* 11/5 (1970) 588

[14] ATIC, http://atic.phys.lsu.edu

[15] CREAM, http://cosmicray.umd.edu/cream/

[16] JACEE, http://marge.phys.washington.edu

[17] RUNJOB, http://runjob.boom.ru/

[18] CGRO, http://heasarc.gsfc.nasa.gov/docs/cgro/cgro/

[19] AGILE, http://agile.rm.iasf.cnr.it

[20] GLAST, http://www.nasa.gov/glast

[21] G. Cocconi, *Handbuch der Physik,* Springer-Verlag, 46/1 (1961) 215

[22] D.Heck, *NEEDS Workshop,* Karlsrhue (2002)

[23] G.V. Kulikov and G.B. Kristiansen, *J.E.P.T.,* 35 (8) (1959) 441

[24] EAS-TOP, http://www.lngs.infn.it/

[25] H. Hayashi et al, *Nucl. Instr. Meth. A,* 545 (2005) 643

[26] KASCADE, KASCADE Grande, http://www-ik.fzk.de/KASCADE_home.html

[27] Ice Top, http://icecube.bartol.udel.edu/

[28] J.Linsley, *Phys.Rev. Lett.,* 10 (1963) 146

[29] M.A. Lawrence et al, *J.Phys. G*, 17 (1991) 733

[30] AGASA, http://www-akeno.icrr.u-tokyo.ac.jp/AGASA/

[31] Pierre Auger Collaboration, http://www.auger.org.ar

[32] MILAGRO, http://www.lanl.gov/milagro

[33] ARGO, http://argo.na.infn.it

[34] MAGIC, http://wwwmagic.mppmu.mpg.de/

[35] VERITAS, http://veritas.sao.arizona.edu/

[36] H.E.S.S., http://www.mpi-hd.mpg.de/hfm/HESS/HESS.html

[37] T.Weekes*, Space Science Reviews,* 75, 1-2, 1-15 (1996)

[38] DUMAND, http://www.phys.hawaii.edu/~dumand

[39] BAIKAL, http://baikalweb.jinr.ru/

[40] ANTARES, http://antares.in2p3.fr/

[41] NESTOR, http://www.nestor.noa.gr/

[42] NEMO, http://nemoweb.lns.infn.it/

[43] ICECUBE, http://www.icecube.wisc.edu/info/

[44] LOPES, http://www.astro.ru.nl/lopes/

[45] CODALEMA, http://codalema.in2p3.fr

PoS(CRA School)027